LBNL-39330
UC-404

CONF-9606237--5

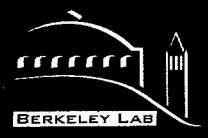

ERNEST ORLANDO LAWRENCE
BERKELEY NATIONAL LABORATORY

Synthesis, Tailored Microstructures and "Colossal" Magnetoresistance in Oxide Thin Films

K.M. Krishnan, A.R. Modak, H. Ju, and P. Bandaru
Materials Sciences Division

September 1996
To be presented at the
International Symposium
"Ceramic Microstructures '96:
Control at the Atomic Level,"
Berkeley, CA
June 24–27, 1996
and to be published in
the Proceedings

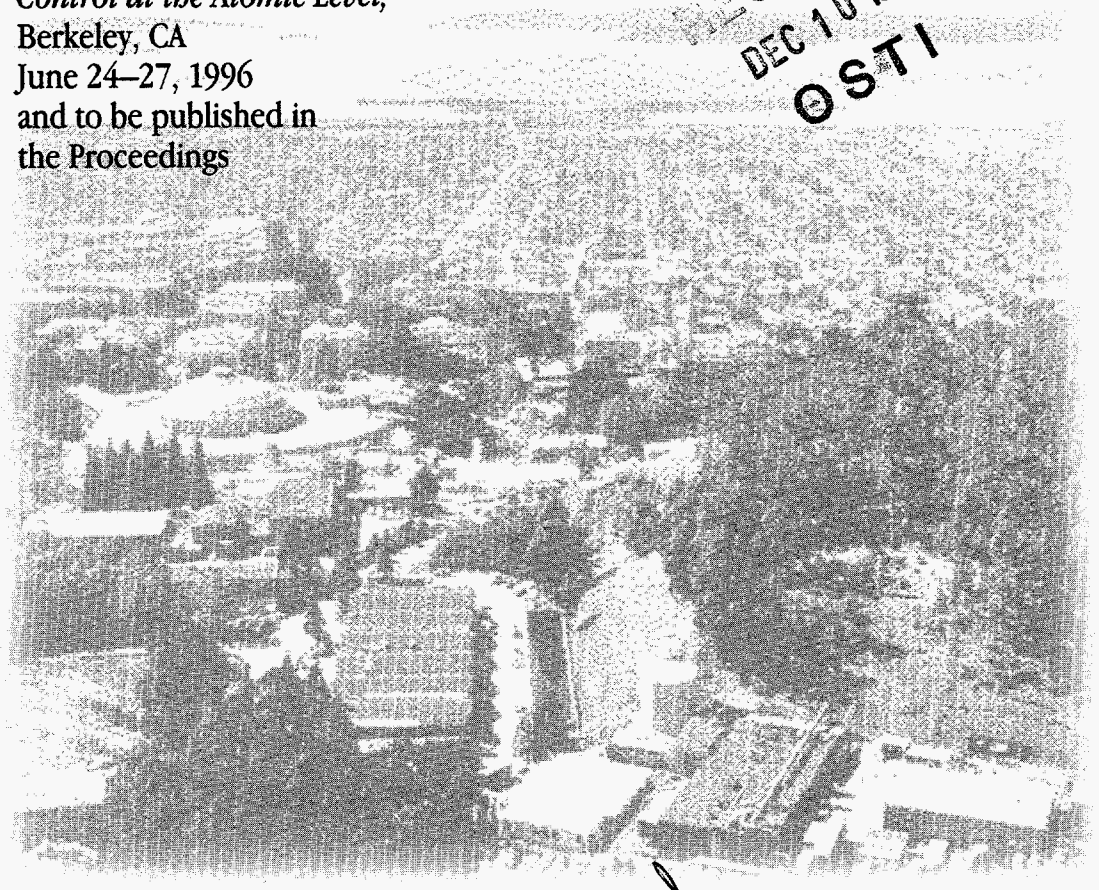

LBNL-39330
UC-404

Synthesis, Tailored Microstructures and "Colossal" Magnetoresistance in Oxide Thin Films

Kannan M. Krishnan, A.R. Modak,* H. Ju, and P. Bandaru

Materials Sciences Division
Ernest Orlando Lawrence Berkeley National Laboratory
University of California
Berkeley, California 94720

September 1996

*Present Address: Silicon Systems, Inc., Santa Cruz, CA

This work was supported by the Director, Office of Energy Research, Office of Basic Energy Sciences, Materials Sciences Division, of the U.S. Department of Energy under Contract No. DE-AC03-76SF00098.

SYNTHESIS, TAILORED MICROSTRUCTURES AND "COLOSSAL" MAGNETORESISTANCE IN OXIDE THIN FILMS

Kannan M. Krishnan[1], A. R. Modak[2] , H. Ju[1] and P. Bandaru[1]
[1]Materials Sciences Divison, E.O. Lawrence Berkeley National Laboratory, Berkeley, CA 94720;
[2]present address, *Silicon Systems Inc.*, Santa Cruz, CA

INTRODUCTION

$La_{1-x}M_x MnO_3$ (where M = Sr, Ba or Ca) thin films, exhibiting very high or "colossal" magnetoresistance (CMR), have generated much recent scientific and technological interest[1-4]. In addition to raising fundamental questions on insulator-metal transitions and magneto-transport phenomenon, these materials have potential impact on the future of magnetic field sensing and data storage devices. However, the magnetic and magneto-transport properties of these manganite thin films are believed to be dependent on the optimization of the conditions of growth/annealing, composition, oxidation state, epitaxy and the overall microstructure.

In order to address these issues we have grown $La_{1-x}Sr_xMnO_3$ ($0<x<1$) films (LSMO) using both pulsed laser deposition and a polymeric sol-gel route developed in our laboratory. Pulsed laser deposition provides the ability to deposit ultra-thin films (1-10 nm) and multilayers in addition to being an established, albeit slower, method for the synthesis of thicker (100-1000nm) perovskite films. Polymeric sol-gel synthesis, if suitably optimized, is very versatile and inexpensive. It has additional advantages of overall simplicity, low processing temperature, ease of composition variation, and the ability to produce a wide range of structures. Overall, these two different growth techniques result in different microstructures but in both cases the texture (epitaxy or polycrystallinity) can be effectively controlled by choice of substrates and growth conditions. The crystallography and microstructure of these films were studied using x-ray difraction and high-resolution transmission electron microscopy. The magnetic/ magnetotransport properties of these LSMO films are then discussed in the context of their growth and microstructural parameters.

THIN FILM GROWTH

LSMO thin films were synthesized[5] by pulsed laser deposition using a 248 nm KrF excimer laser (Lambda Physik, Lextra 200) with a 30ns pulse width and output energy of

400 mJ. The laser was operated at 3 Hz for 15 minutes producing films ~50nm thick. A sintered $La_{0.8}$ $Sr_{0.2}$ MnO_3 target was used. The ejected plume of material was deposited simultaneously onto polished $LaAlO_3$[100] and Si[100] (with native oxide) substrates maintained at 675°C. The base pressure in the chamber was $2x10^{-6}$ Torr. During the deposition the oxygen pressure in the vacuum chamber was maintained at 100 mTorr by flowing oxygen at 50-70 sccm. After deposition, the films were cooled to room temperature at 5°C/min. in an oxygen pressure between 500-600 Torr.

The polymeric chemical process developed in our laboratory [6] used organometallic precursors of the constituent elements which were synthesized from commercially available compounds. Alkoxides of La, Sr and Mn are possible starting materials due to their ability to complex into atomically well-mixed precursors[7]. However, alkoxides of lanthanum and manganese have limited solubility in organic solvents and hence their respective carboxylates or β-diketonates, were used. Strontium metal, can be readily reacted with different alcohols to form stable alkoxides which are completely soluble in the respective alcohols. After several such considerations and pilot experiments we arrived at lanthanum 2,4-pentanedionate (or Lanthanum acetyl acetonate), manganese(II) acetate and strontium methoxyethoxide as the organometallic precursors. 2-methoxyethanol was used as the base solvent since it has been reported to have advantages over other alcohols in similar sol-gel processes for fabricating perovskite thin films. Individual precursors underwent further processing steps of complexation (in required stoichiometric proportions, i.e. La:Sr:Mn = 0.8:0.2:1) and hydrolysis. To estimate and optimize hydrolysis the precursor complex was hydrolysed, in a pilot experiment, using varying amounts of water from 1 mole H_2O/mole manganese to 3 moles H_2O/mole manganese. Instead of carrying out gelation tests, each solution was aged for one day and films were deposited. X-ray diffraction was carried out on all the films to determine occurence of extraneous phases resulting from variation in hydrolysis conditions but no difference in the crystal structure was observed for the above range of conditions. This is not unusual because it has been observed before that β-diketonate ligands hydrolyse very slowly, in effect making this process hydrolysis independent.

The complex solutions were spin cast (2000 rpm, 30 sec.) on the required substrate ($LaAlO_3$(100) or Si(100)) accompanied by solvent removal at 300°C. Thermogravimetric analysis (TGA) of the gel dried at a low temperature (80°C) was carried out to estimate film heat treatment temperature. Fig. 1 shows a plot of the weight of the sample versus temperature from the TGA experiment carried out at a heating rate of 10°C/min. The plot reveals an initial gradual weight loss at low temperatures related to solvent removal,

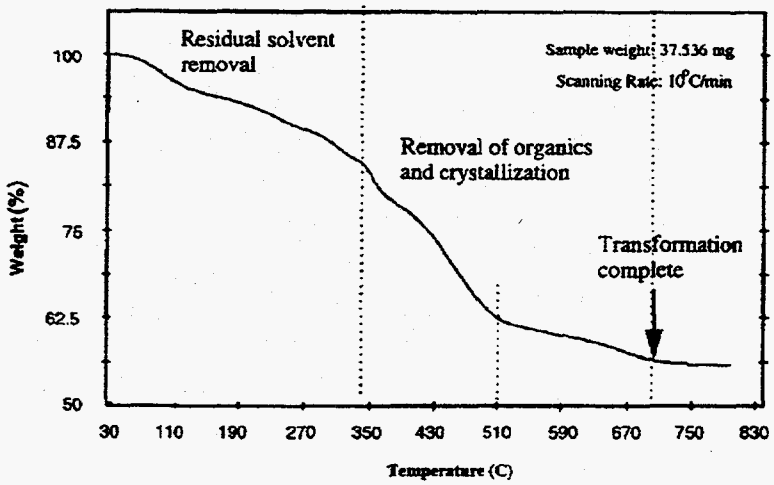

Figure 1. Thermogravimetric analysis of precursor complex gel: weight as a function of temperature measured during heating cycle from 0 - 800 °C at 10°C/min.

followed by a rapid weight loss between 350 and 500°C which is associated with the oxidation of the organics with release of CO_2 and H_2O. There is further gradual weight loss after 500°C (about 10% of total weight loss) and the weight remains constant after about 650°C at which temperature the organometallic-to-oxide conversion was presumed to be complete. The solution was spin cast at 2000 rpm for 30 seconds on the required substrates (either Si(100) or $LaAlO_3$(100)) to form an amorphous condensed film. Amorphous films were heated at 300°C on a hot plate, immediately after spin coating, for trapped solvent removal. Final heat treatment was carried out, based on the above TGA results, at 700°C for 1 hour in air to obtain the oxide thin films. Multiple deposition/drying cycles were used to make thicker films.

CHARACTERIZATION: CRYSTALLOGRAPHY AND MICROSTRUCTURE

PLD grown $La_{0.8}Sr_{0.2}MnO_3$ Thin Films

Figures 2 a&b show x-ray scans from the LSMO(80/20) films on Si(100) and $LaAlO_3$(100) substrates respectively. A fixed θ (~ 8°), variable 2θ scan (Fig. 2a) of the film grown on Si(100), confirms it to be polycrystalline and randomly oriented. Assuming a cubic structure for the perovskite film, the peaks were indexed as shown and the lattice constant was determined to be a = 3.88 ± 0.05Å. Fig. 2b shows a conventional θ–2θ scan for the film grown on the $LaAlO_3$ substrate (a=3.78Å). The split peaks at each position correspond to the substrate (higher intensity) and the perovskite film. The position of the perovskite peak corresponds to a cubic surface-normal lattice constant, c = 3.92 Å. Measurement of in-plane Bragg reflections, e.g. (111), gave a smaller lattice mismatch and implies that there is some in-plane lattice matching causing a tetragonal distortion in the epitaxial film. The shoulder on the low angle side of the film peak (fig. 2b) is an order of magnitude smaller than the principal peak and may be due to regions of the film that are perfectly lattice matched, in-plane, to the substrate, thus leading to a larger tetragonal distortion.

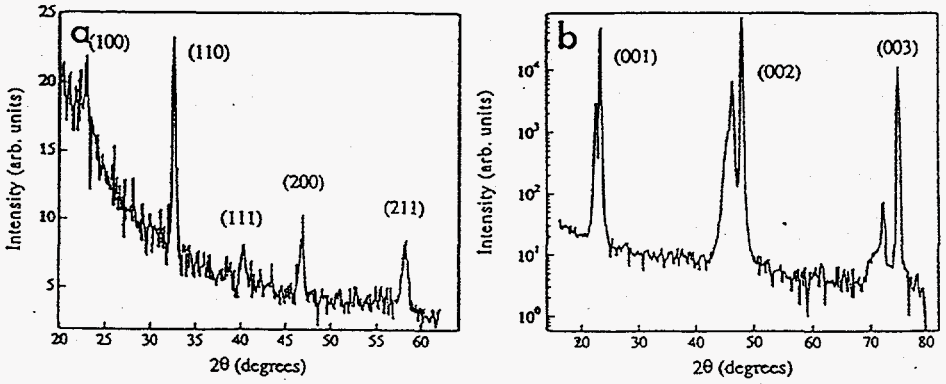

Figure 2. X-ray diffraction data of PLD grown LSMO films on (a) Si(001) and (b) $LaAlO_3$(001)

Transmission electron micrographs of the PLD grown LSMO(80/20) film, on Si(100) substrate, are shown in Fig. 3a &b. In plan view, the film is seen to be polycrystalline with a grain size of 100-200 nm. In cross-section, the films is revealed to be uniform, ~ 450Å thick and having columnar grain morphology. The film/substrate interface was found to be

free of interdiffusion. The SAD pattern (Fig. 3c) shows a diffraction ring which was indexed to a cubic structure with the same lattice parameters as those observed from XRD.

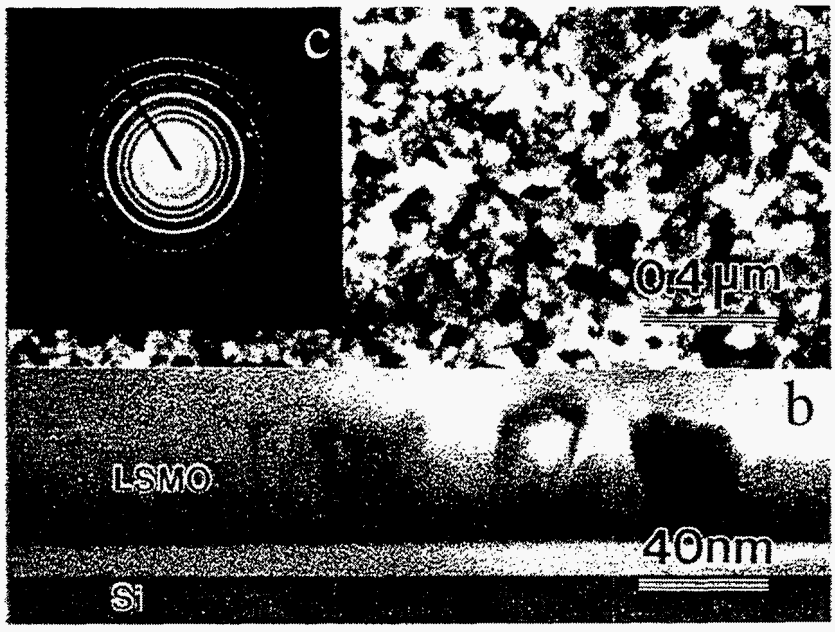

Figure 3. Transmission electron microscopy of LSMO films grown on Si(001) -- (a) plan view, (b) cross-section and (c) selected area diffraction.

Sol-gel Derived $La_{1-x}Sr_xMnO_3$ (0< x< 0.7) Thin Films

The thin films had a smooth reflecting surface and were completely crack-free. The crystal structure was investigated using x-ray diffraction (XRD). Fig. 4(a) and(b) show normal θ/2θ scans taken from LSMO(80/20) thin films grown on Si(100) and $LaAlO_3$(100) substrates respectively. Single phase, polycrystalline and randomly oriented $La_{0.8}Sr_{0.2}MnO_3$ thin films were obtained on Si(100) substrates. The XRD pattern from films grown on the LaAlO3 substrate clearly revealed that the films were highly oriented. Diffraction peaks corresponding to only (100) and (200) crystal planes were observed in the normal θ/2θ scans indicating complete (100) normal epitaxy. A plan view, bright field transmission electron micrograph (Fig. 5a) of the LSMO(80/20) thin film grown on Si(100) shows the polycrystalline microstructure with a grain size of 1-2 μm and some inter- and intra-granular porosity (10-20%). In cross-section (Fig. 3b), the film was confirmed to be 0.5μm thick and uniform with some surface roughness (~20 nm). The multilayer structure arising from the multiple coatings (to build film thickness) is distinctly visible. Similar to the PLD films, there was little evidence of interdiffusion at the film/substrate interface. The selected area electron diffraction pattern (Fig. 5c) was indexed to a cubic structure with the same lattice parameters as observed from XRD.

MAGNETIC AND TRANSPORT PROPERTIES

PLD grown $La_{0.8}Sr_{0.2}MnO_3$ Thin Films

The magnetization M(T, H= 5 kOe) data (Fig. 6a) for the two films shows that their ferromagnetic transition temperatures are different (T_c=180K($LaAlO_3$); T_c=230K (Si)). At

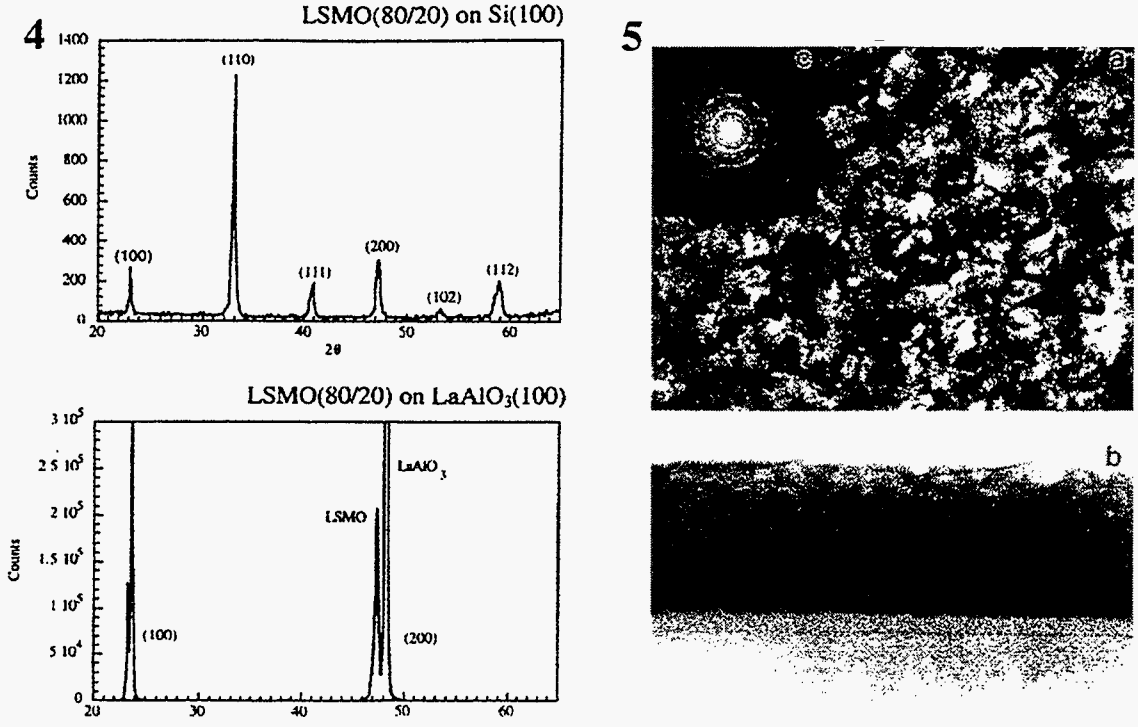

Figure 4. θ–2θ x-ray scans for LSMO films grown on (a) Si(001) and (b) $LaAlO_3$(001)
Figure 5: TEM of polycrystalline LSMO films grown by the sol-gel process on Si(001) -- (a) plan view, (b) cross-section and (c) selected area diffraction.

room temperature, both films show a M(H) behaviour that is linear with applied field consistent with antiferromagnetism (Fig. 6b & c). However, the magnetic moment at 5T for the polycrystalline film (≈0.0035 emu) is higher than that observed for the epitaxial film (≈0.0022 emu). At 10K, both films showed a non-linear hysteresis indicative of their ferromagnetic nature along with a significant high field slope even at applied fields of 5T.

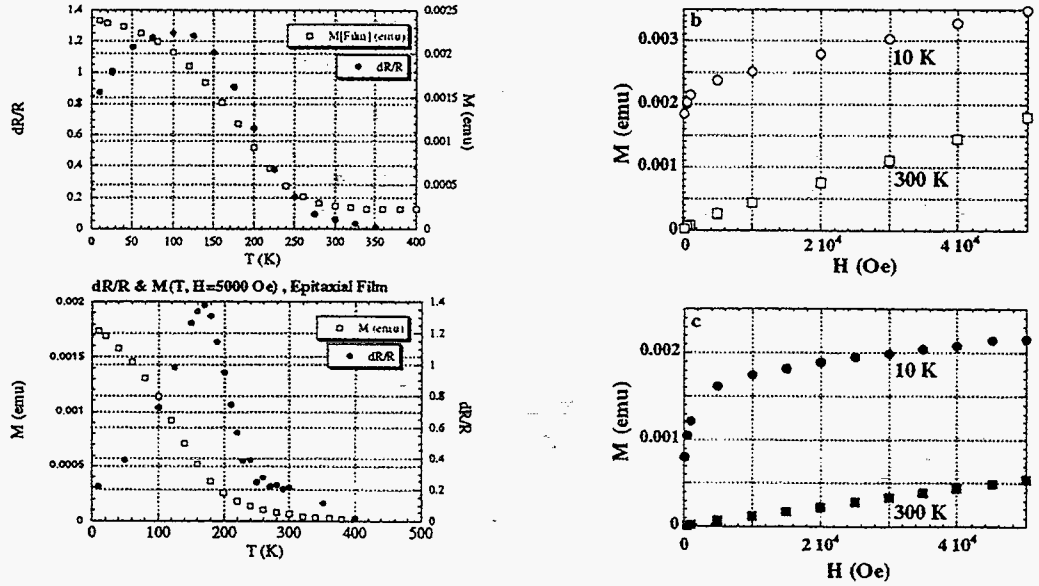

Figure 6: Magnetization data for LSMO(80/20) thin films: (a) M vs T for polycrystallinae and epitaxial films (b) M vs H for polycrystalline film and (c) M vs. H for epitaxial film

The temperature and field dependent resistance values of the films grown on the two different substrates were also different. The overall resistance of the polycrystalline films on Si was 2-3 orders of magnitude greater than that of the single crystal film on $LaAlO_3$. The resistance of the polycrystalline film increased monotonically with decreasing temperature except for a small bump observed around 130K (Fig.7a). At roughly the same temperature, a rather broad peak in the magnetoresistance was observed; the peak magnetoresistance was 125% in a field of 5T. The zero-field resistance of the single crystal film peaked (at 185K) more sharply than the polycrystalline films, and dropped as temperature decreased further indicating a semi-conductor to metal transition (Fig. 7b). In this case, the peak in magnetoresistance correlates reasonably well with the onset of the magnetic transition; the peak magnetoresistance of the single crystal was 140% in a field of 5 T, at a temperature of 170K, which is slightly below the magnetic transition.

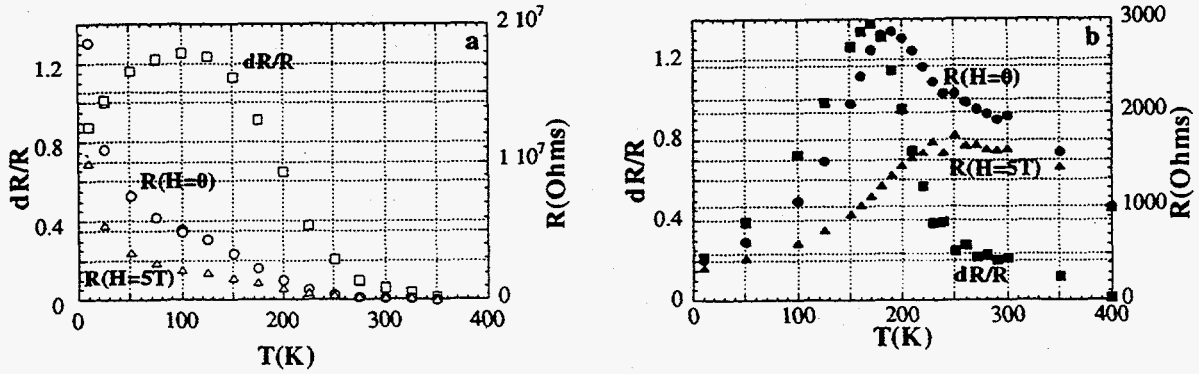

Figure 7. Resistivity data for PLD grown films at H = 0 and 5T: (a) polycrystalline; (b) epitaxial

Sol-gel Derived $La_{1-x}Sr_xMnO_3$ (0< x< 0.7) Thin Films

The ability to make any composition, rapidly and reproducibly, either epitaxial or polycrystalline, allows us to study the entire composition range with ease. Fig. 8 shows zero-field resistivity data as a function of temperature for a wide range of LSMO compositions grown epitaxially on $LaAlO_3$. Except for an intermediate range of compositions ($0.2 \leq x \leq 0.4$) the films are insulating at all temperatures. For x=0.2, one can clearly observe an insulator to metal transition at ~260 K and for x=0.3, the onset of the transition at 350K is clearly evident.

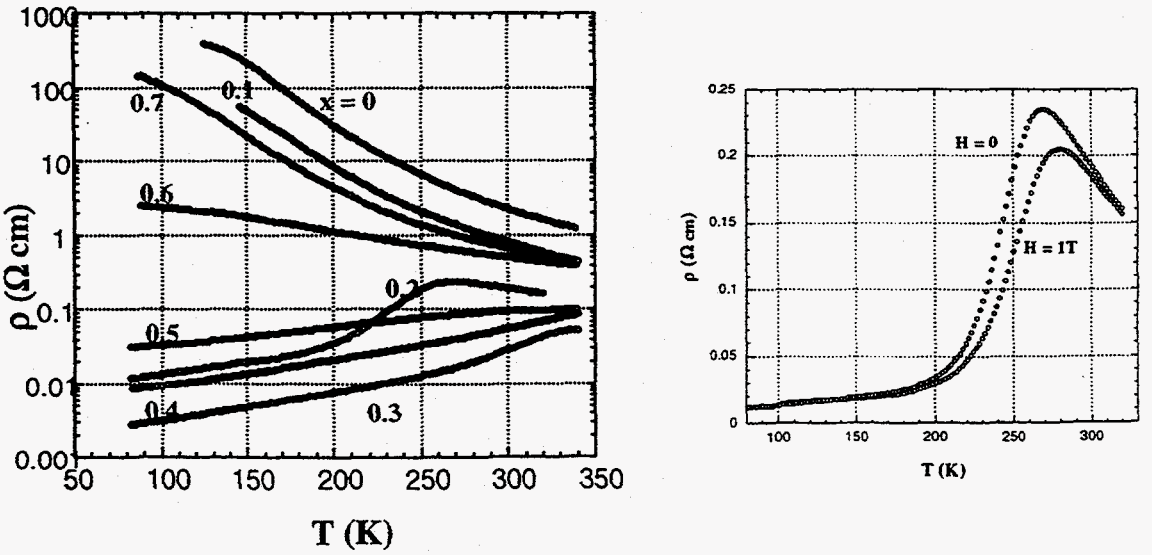

Figure 8: Zero- field resistivity data for the entire range of LSMO compositions grown on $LaAlO_3$

Figure 9: Resistance (at H=0 and 1T) as a function of temperature .

Resistance measurements as a function of temperature (Fig. 9) with H=0 for an optimally annealed LSMO(80/20) thin film grown on $LaAlO_3$(100) show a distinct peak at ~260 K. At H=1T, the peak is supressed substantially and undergoes a shift to higher temperature. In general, the zero field resistance of the polycrystalline films was an order of magnitude higher than the epitaxial films (500 kOhms as opposed to 25 kOhms), similar to the PLD grown films. The epitaxial thin films exhibit a peak MR of 88% at an applied field of 1T.

DISCUSSION

For both growth methods, the choice of substrate determines the orientation of the LSMO film. The Si(100) substrates, with a ~10nm thick oxide layer, imposes no crystallographic constraints on the nucleating phase and leads to polycrystallinity and random orientation. In the case of $LaAlO_3$, the nucleation is strongly influenced by the surface which constrains the films to have an epitaxial relationship. Thus the crystallographic texture is primarily determined by the substrate surface template.

The PLD grown polycrystalline films have a grain size (100-200nm) which is comparable to the film thickness. This is expected since the substrate is held at 675°C providing considerable surface mobility during growth to the incoming atoms. The mechanism, however, is quite different in sol-gel derived thin films -- the grain size in the film is determined not only by the growth kinetics but also by the nature of the polymeric condensed gel[8]. The relatively large grain size ($\approx$ 1-2 μm) observed is a reflection of considerable crosslinking and formation of large colloidal units in the amorphous spun-coat films and their subsequent crystallization into large individual grains. The high porosity (10-20%) is left after removal of the organic mass after which there is very little diffusion-induced densification[8]. Observation of individual layers in the multicoated sol-gel film indicates that preliminary crystallization probably occurs during low temperature solvent removal.

For both PLD and sol-gel derived films, the resistivities of the polycrystalline films are much higher than the corresponding epitaxial films. This can be explained on the basis of the additional scattering from defects and grain boundaries in polycrystalline as opposed to epitaxial films. The differences in transition temperature of LSMO films of identical composition, but grown by these two techniques, could be related to differences in thickness, microstructure as well as composition (oxygen stoichiometry and local compositional inhomogeneties). The differences in the magnitude of magnetoresistance between polycrystalline and epitaxial films is more pronounced for sol-gel films which could be due to their higher thickness (0.5μm as opposed to 450Å for PLD grown fims). However, the cause for the MR enhancement with epitaxy is again related to both morphological and compositional effects and is still not completely understood.

The magnetic moment differences at room temperature between the epitaxial and polycrystalline films can be qualitatively explained. In single crystal LSMO, alternate (001) planes are antiferromagnetically ordered with the moments ferromagnetically ordered along either the [010] or the [100] directions. Hence for an (100) epitaxial film, with the field applied in the plane of the film and assuming that the two spin orientations are equally distributed, the measured susceptibility is: $\chi_{epitaxial} = 1/2\ (\chi_{//} + \chi_{\perp})$ where $\chi_{//}$ and $\chi_{\perp}$ are the susceptibilities parallel and perpendicular to the spin alignment. At the same time, for the polycrystalline film, the measured susceptibility is $\chi_{polycrystalline} = 1/3\ (\chi_{//} + 2\chi_{\perp})$ assuming random orientation[9]. Below the Neel temperature, since $\chi_{//} < \chi_{\perp}$, the polycrystalline film would have a higher measured susceptibility than the (100) epitaxial film. The low temperature magnetic moment differences, however, are rationalized on the basis of

possible differences in the amount of Mn^{4+} ions between polycrystalline and epitaxial thin films which in turn affects the moment per Mn atom [10]. The non-equilibrium oxygen content of polcrystalline materials can be expected to be higher than epitaxial films due to enhanced diffusion through grain boundaries, which would force a higher Mn^{4+} to maintain the charge balance. Efforts to quantify the Mn^{4+}/Mn^{3+} ratios in the films utilizing electron energy loss spectroscopy and soft x-ray spectroscopy are currently in progress.

Both the Curie temperature and the ferromagnetic magnetization of the epitaxial film are lower than those of the polycrystal implying that the ferromagnetic moment per Mn atom is smaller in the single crystal than in the polycrystal. In these films the relative atomic fraction of both Sr and O affect the tetravalent Mn content. Further, the change in the ferromagnetic moment per Mn atom with the fraction of tetravalent Mn is particularly large close to 20% Mn^{4+}, which would be expected in the composition corresponding to 20 at. % Sr [2]. Since the total number of La, Sr and Mn atoms in the two films are nominally equal, the difference in the moments could arise mainly from differences in oxygen stoichiometry. The interdiffusion of oxygen would be much faster along grain boundaries than in the bulk and hence, the polycrystal would have a higher equilibrium oxygen content than the single crystal. Future EELS measurements may help to clarify the issue relating to the relative oxygen stoichiometries in the two films.

Overall, the results confirm the important role of the microstructure in determining the properties of LSMO films and suggest the need to make measurements on well defined grain boundaries, e.g. films grown on bicrystal substrates. Such experiments would permit an understanding of the influence of grain boundaries on the double exchange interactions, in addition to magnetoresistance properties.

ACKNOWLEDGEMENTS

This work was supported by the Director, Office of Energy Research, Office of Basic Energy Sciences, Materials Sciences Division of the U.S. Department of Energy under contract no. DE-AC03-76SF00098.

REFERENCES

1. K. Chahara, T. Ohno, M. Kasai and Y. Kozono, Appl. Phys. Lett **63**, 1990 (1993).
2. R. von Helmolt, J. Wecker, B. Holzapfel, L. Schultz and K. Samwer, Phy. Rev. Lett. **71**, 2331 (1993).
3. S. Jin, M. McCormack, T. H. Tiefel and R. Ramesh, J. Appl. Phys. **76**, 6929 (1994).
4. Refer to Proceedings of the 50th MMM Conference, Philadelphia, PA, November 1995.
5. Kannan M. Krishnan, A. R. Modak, C. A. Lucas, R. Michel and H. B. Cherry, J. Appl. Phys., **79**, 5169 (1996)
6. A. R. Modak and Kannan M. Krishnan, J. Amer. Ceram. Soc., 1995, In Press.
7. A. R. Modak and S. K. Dey, Integrated Ferroelectrics 5, 321 (1994).
8. C. J. Brinker and G. W. Scherer, *Sol-Gel Science: The Physics and Chemistry of Sol-Gel Processing*, (Academic Press, Boston, 1990)
9. B. D. Cullity, *Introduction to Magnetic Materials* (Addison-Wesley, Reading MA, 1972).
10. G. H. Jonker and J. H. van Santen, Physica **16**, 337 (1950)